

# Balancing of a linear elastic rotor-bearing system with arbitrarily distributed unbalance using the Numerical Assembly Technique

Georg QUINZ\*, Marcel S. PREM, Michael KLANNER, and Katrin ELLERMANN

Graz University of Technology, Institute of Mechanics, Kopernikusgasse 24/IV, 8010 Graz, Austria

**Abstract.** In this paper, a new application of the Numerical Assembly Technique is presented for the balancing of linear elastic rotor-bearing systems with a stepped shaft and arbitrarily distributed mass unbalance. The method improves existing balancing techniques by combining the advantages of modal balancing with the fast calculation of an efficient numerical method. The rotating stepped circular shaft is modelled according to the Rayleigh beam theory. The Numerical Assembly Technique is used to calculate the steady-state harmonic response, eigenvalues and the associated mode shapes of the rotor. The displacements of a simulation are compared to measured displacements of the rotor-bearing system to calculate the generalized unbalance for each eigenvalue. The generalized unbalances are modified according to modal theory to calculate orthogonal correction masses. In this manner, a rotor-bearing system is balanced using a single measurement of the displacement at one position on the rotor for every critical speed. Three numerical examples are used to show the accuracy and the balancing success of the proposed method.

**Key words:** Numerical Assembly Technique; rotor dynamics; modal balancing; recursive eigenvalue search algorithm.

## NOMENCLATURE

|                    |  |
|--------------------|--|
| $A$                | area of segments ( $m^2$ )                                   |
| $\underline{A}$    | amplitude matrix   |
| $c$                | spring constant (N/m)  |
| $d$                | damping constant (Ns/m)                                      |
| $E$                | Young's modulus (N/m <sup>2</sup> )                          |
| $I$                | second moment of area about $x$ - and $y$ -axis ( $m^4$ )    |
| $m$                | external distributed moments (N)                             |
| $M$                | bending moment (Nm)  |
| $q$                | external distributed forces (N/m)                            |
| $Q$                | shear forces (N)   |
| $t$                | time (s)   |
| $\vec{U}$          | unbalance vector (kg m)                                      |
| $z$                | axial position (m)   |
| $\beta$            | angle of eccentricity (rad)                                  |
| $\varepsilon$      | amount of eccentricity (m)                                   |
| $\Theta$           | angular mass about $x$ - and $y$ - axis (kg m <sup>2</sup> ) |
| $\rho$             | density (kg/m <sup>3</sup> )                                 |
| $\varphi$          | rotation of cross section (rad)                              |
| $\underline{\phi}$ | modal matrix   |
| $\Omega$           | spin speed (rad/s)   |

## 1. INTRODUCTION

Rotary machines often encounter excessive vibrations due to rotating unbalance. If the operating speed exceeds 70% of the first flexural critical speed, a rotor system is considered flexi-

ble and the displacement of the shaft cannot be neglected [1]. The goal of flexible balancing is to minimize the elastic displacement of the rotor throughout the whole length of the shaft and all operating speeds. There are two groups of methods for the balancing of flexible rotors: influence coefficient methods and modal balancing methods. The *influence coefficient method* does not require any assumptions, except the linearity of the rotor and measurement system, but needs a large number of test runs. The *modal balancing method* requires only a small set of test runs and is accurate up to higher modes. However, it is necessary to know the mode shapes of the system to calculate the orthogonal weight sets [2].

There are different methods to find these weight sets: intuitive [3], experimental [4] and numeric methods [5]. This paper presents a new numeric modal balancing method. The *Transfer Matrix Method* (TMM) is a common technique to find the eigenvalues and the unbalance response necessary for balancing. Lee *et al.* [6] generalized the classical TMM and included distributed unbalances in the calculation using Fourier series representation instead of lumped parameter models. An extension of this method is the *Numerical Assembly Technique* (NAT). In its original form introduced by Wu and Chou [7], it is applicable for harmonic vibrations of one-dimensional structures. In recent years, the method has been extended to calculate the whirling speed and the mode shape of rotor models according to the Euler-Bernoulli beam theory [8] and Rayleigh beam theory [9]. Distributed loading has been introduced by Klanner and Ellermann [10]. NAT is a very powerful tool to investigate the behaviour of rotor-bearing systems since it leads to quasi analytical solutions and it is computationally more efficient than the Finite Element Method (FEM) [9]. In this paper the NAT method according to Rayleigh beam theory devel-

\*e-mail: gquinz@tugraz.at

Manuscript submitted 2021-03-26, revised 2021-05-25, initially accepted for publication 2021-06-12, published in December 2021

oped by Klanner *et al.* [9] is used to simulate rotor-bearing systems and thus transfer the benefits of NAT to a modal balancing method.

## 2. BALANCING METHOD

The proposed method uses measurements from one rotor-bearing system in different states of unbalance. The setup of a rotor measurement test bed is shown in Fig. 1.

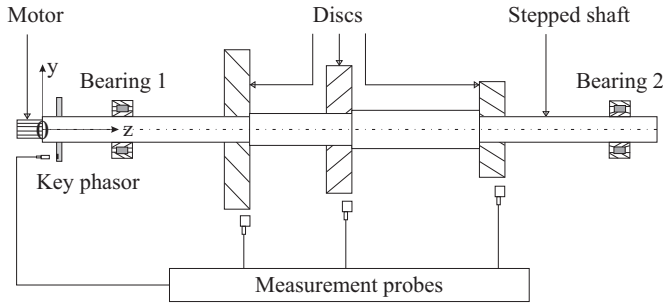


Fig. 1. Rotor-bearing measurement system (adapted from [11])

The displacement of the rotor is determined by measurement probes and the angular position by a photosensitive sensor, commonly referred to as key phasor.

The first set of measurements is taken in the initial state of the system before balancing. Measurements of vibrations at every critical speed up to the operating speed are taken. Furthermore, the geometric parameters and material properties of the initial system are used to simulate a digital model, which is excited by a standardised unbalance.

The second state is described by this digital model. It is used to determine eigenvalues, mode shapes and the unbalance response at critical speeds caused by a known unbalance. Due to these values, an orthogonal weight set for each mode shape can be found.

The rotor is balanced by mounting the compensation weights. By comparing the vibration levels of the system in its balanced and in its initial state, the balancing success is evaluated. The steps are summarised in Fig. 2.

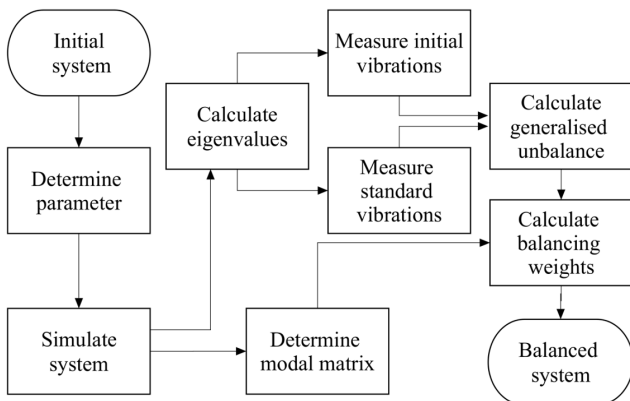


Fig. 2. Flowchart of the balancing process

## 2.1. Simulation

The rotor system is simulated using the Numerical Assembly Technique. The main advantages of this technique are the quasi-analytical solutions and its low computational effort. In [9], numerical comparisons show a reduction of the computational time by a factor of ten compared to FEM. Each rotor segment is modelled according to the Rayleigh beam theory, which is based on the same assumption as the Euler-Bernoulli beam theory, but includes rotary inertias and gyroscopic effects [9, 12]. The space fixed coordinate system  $Oxyz$  is chosen, so that  $Oz$  passes the undeflected axis of the rotor in its bearings.  $Ox$  and  $Oy$  are perpendicular to each other and transverse to  $Oz$ . The state of the rotor is described by the displacements  $u_x$  and  $u_y$ , the rotations of the cross section  $\varphi_x$  and  $\varphi_y$ , the bending moments  $M_x$  and  $M_y$  and the shear forces  $Q_x$  and  $Q_y$ . The equilibrium of forces and moments on an infinitesimal rotor element leads to the equations of motion

$$EI \frac{\partial^4 u_x(z,t)}{\partial z^4} - \rho I \frac{\partial^4 u_x(z,t)}{\partial z^2 \partial t^2} + \rho A \frac{\partial^2 u_x(z,t)}{\partial t^2} - 2\rho I \Omega \frac{\partial^3 u_y(z,t)}{\partial t \partial z^2} - \frac{\partial m_y(z,t)}{\partial z} + q_x(z,t) + \rho A \varepsilon(z) \Omega^2 \cos(\Omega t + \beta(z)), \quad (1a)$$

$$EI \frac{\partial^4 u_y(z,t)}{\partial z^4} - \rho I \frac{\partial^4 u_y(z,t)}{\partial z^2 \partial t^2} + \rho A \frac{\partial^2 u_y(z,t)}{\partial t^2} + 2\rho I \Omega \frac{\partial^3 u_x(z,t)}{\partial t \partial z^2} - \frac{\partial m_x(z,t)}{\partial z} + q_y(z,t) + \rho A \varepsilon(z) \Omega^2 \sin(\Omega t + \beta(z)), \quad (1b)$$

where  $E$  is the Young's modulus,  $I$  is the second moment of area of the cross section about the  $x$ - and  $y$ -axis,  $\rho$  is the density,  $\Omega$  is the spin speed,  $m_\bullet$  are the external distributed moments,  $q_\bullet$  are the external distributed forces,  $A$  is the area of the cross-section,  $\varepsilon$  is the amount of eccentricity and  $\beta$  is its angular position [9]. The rotations of the cross section are defined by

$$\varphi_y(z,t) = \frac{\partial u_x(z,t)}{\partial z}, \quad (2a)$$

$$\varphi_x(z,t) = -\frac{\partial u_y(z,t)}{\partial z}, \quad (2b)$$

the bending moments are defined by

$$M_y(z,t) = EI \frac{\partial^2 u_x(z,t)}{\partial z^2}, \quad (3a)$$

$$M_x(z,t) = -EI \frac{\partial^2 u_y(z,t)}{\partial z^2} \quad (3b)$$

and the shear forces can be computed by

$$Q_x(z,t) = \rho I \frac{\partial^3 u_x(z,t)}{\partial t^2 \partial z} + 2\rho I \Omega \frac{\partial^2 u_y(z,t)}{\partial t \partial z} - EI \frac{\partial^3 u_x(z,t)}{\partial z^3} - m_y(z,t), \quad (4a)$$

$$Q_y(z,t) = \rho I \frac{\partial^3 u_y(z,t)}{\partial t^2 \partial z} - 2\rho I \Omega \frac{\partial^2 u_x(z,t)}{\partial t \partial z} - EI \frac{\partial^3 u_y(z,t)}{\partial z^3} + m_x(z,t). \quad (4b)$$

The proposed method assumes a solution of the form

$$u_x(z,t) = \tilde{u}_x^+(z)e^{i\Omega t} + \tilde{u}_x^-(z)e^{-i\Omega t}, \quad (5a)$$

$$u_y(z,t) = \tilde{u}_y^+(z)e^{i\Omega t} + \tilde{u}_y^-(z)e^{-i\Omega t}, \quad (5b)$$

which leads to four ordinary differential equations. The differential equations for  $u^+(z)$  and  $u^-(z)$  are completely decoupled, since the solutions of  $u^+(z)$  and  $u^-(z)$  have to be complex conjugated to yield the real solutions for  $u(z,t)$ . Therefore only two of these equations

$$\frac{\partial^4 \tilde{u}_x^+(z)}{\partial z^4} + \rho \Omega^2 \frac{\partial^2 \tilde{u}_x^+(z)}{E \partial z^2} - \frac{\rho A \Omega^2}{EI} \tilde{u}_x^+(z) - 2i\rho \Omega^2 \frac{\partial^2 \tilde{u}_y^+(z)}{E \partial z^2} = \frac{\rho A \Omega^2}{2EI} \varepsilon(z)e^{i\beta(z)}, \quad (6a)$$

$$\frac{\partial^4 \tilde{u}_y^+(z)}{\partial z^4} + \rho \Omega^2 \frac{\partial^2 \tilde{u}_y^+(z)}{E \partial z^2} - \frac{\rho A \Omega^2}{EI} \tilde{u}_y^+(z) + 2i\rho \Omega^2 \frac{\partial^2 \tilde{u}_x^+(z)}{E \partial z^2} = -\frac{i\rho A \Omega^2}{2EI} \varepsilon(z)e^{i\beta(z)}, \quad (6b)$$

are necessary. An approach similar to Wu *et al.* [8] would also result in equivalent system equations. In NAT, analytical solutions of the governing equations (6) are used to fulfil the boundary and interface conditions. The particular solutions include concentrated and generally distributed unbalances. The assembly of the total solutions of each rotor segment leads to a system of linear equations [9, 12].

For a detailed description of the boundary conditions and the assembly process, the reader is referred to Klanner *et al.* [9].

The parameters necessary to describe the rotor-bearing system are split into two groups: station- and segment-parameters. Stations separate segments and represent bearings, discs or steps in the rotor. They are described by up to ten parameters: axial position, mass, angular mass about  $x$ - and  $y$ - and about  $z$ -direction, eccentricity of discs and the angular position of this eccentricity and spring and damping coefficient in each direction for the description of bearings. Setting parameters of the disc or bearing to zero facilitates every possible configuration at the stations [9]. The spring and damper constants of the bearings are not necessarily equal in both directions, therefore the simulation of anisotropic behaviour is possible. Since this paper focuses on modal balancing of isotropic rotor systems, this behaviour is not yet included. Segments are cylinder elements between these stations. They are described by four parameters: Young's modulus, density, area of cross section and second moment of cross section area. The simulation of the rotor-bearing system with standard imbalance assumes that the rotor is excited by a single concentrated imbalance. As the system is linear, the magnitude and position of the imbalance can be chosen

arbitrarily. We use a standard imbalance of 1 kgm at the  $0^\circ$  position of a cross section. It is important that the position in axial direction is not on a node of one of the considered bending modes.

All measurements are taken according to the *N plane method* [13]: If the system is to be balanced in the first  $N$  bending modes, it needs to be balanced at  $N$  positions. When the forms of the bending modes are known, only the amplitude and phase angle of the displacement on a single position on the rotor are needed. Nodes of the eigenmodes have to be excluded. Every measurement is taken using a single test run without trial masses. Additional measurements can be used to compensate for measurement errors with the least squares method. The vibrations of the rotor are measured for each relevant critical speed. The amplitudes and the angle of maximum displacement of each measurement are combined in one complex value, where the displacement in  $x$ -direction corresponds to the real part and the displacement in  $y$ -direction to the imaginary part. The complex values of all measurements are gathered in the amplitude matrix of the initial system  $\underline{A}_I$ . The amplitude matrices for the standardised system  $\underline{A}_S$  and for the balanced system  $\underline{A}_B$  are formed in the same manner. In the matrix  $\underline{A}_I$ , one entry per critical speed is sufficient for balancing. The matrix  $\underline{A}_S$  has to be fully populated to determine the mode shapes and the modal matrix. Since these values are calculated by the NAT simulation, there is no associated measurement effort. To be able to compare the balancing success, the matrix of the balanced system  $\underline{A}_B$  has to be populated the same way as  $\underline{A}_I$ .

In this paper, the measurements of the real and balanced system are simulated using the FEM software package ANSYS® 2019R2. This facilitates the testing of the proposed balancing method for many different cases.

## 2.2. Recursive eigenvalue search

At every critical speed, the coefficient matrix of the Transfer Matrix Method and also of the NAT model is singular [14]. Usually, the singularity of a matrix is checked by its determinant to be zero [15]. For this a modification of a numeric recursive eigenvalue search algorithm developed by Bestle *et al.* [16] is used. This algorithm reduces the zero search to a minimization problem, which is more robust and can be solved faster. Classical root search strategies look for a change of the sign of the determinant of the coefficient matrix. This can be problematic when two zeros are close to each other or in the case of double roots. If the step size is too big, these eigenvalues might be overlooked. The method of Bestle *et al.* [16] solves this problem by searching for local minima in the absolute value of the determinant of the coefficient matrix. It is also a recursive algorithm: Every time a local minimum of the function is found, the algorithm is repeated in an area of one step size in both directions around the lowest value, until the desired accuracy is met. Since the space between critical speeds usually increases with higher frequencies, the algorithm searches in logarithmic steps instead of linear ones. In the case of a damped rotor-bearing system, the eigenvalues are complex numbers and the zero search problem depends on two variables, the damped critical speed  $\omega_d$  and the modal damping coefficient  $d$ . In this case, the algorithm

searches a matrix of those two variables for values, which are a minimum in both directions and repeats this process until the desired accuracy is met [16].

### 2.3. Modal balancing

The proposed method builds on the *N plane method*. In this method, the modal components of imbalance are corrected in a progressive way in the vicinity of critical speeds without affecting already balanced modes [13, 17]. The modal matrix is needed to find orthogonal balancing weights that influence only a single mode shape. It consists of the relations of displacements of the rotor on each critical speed and at each measure position. Since the matrix of the real system might not be completely filled, the matrix of the simulated model  $\underline{A}_S$  is used. It is made non-dimensional to get the modal matrix  $\underline{\phi}$ . The requirement for perfect balance is the vanishing of displacements on all measurement points. The exciting unbalances consist of two parts: an initial unbalance  $\vec{U}_I$  and an imbalance mounted for compensation  $\vec{U}_C$ . The equation

$$\underline{\phi}^T \vec{U}_C = -\underline{\phi}^T \vec{U}_I \quad (7)$$

is fulfilled for a completely balanced system. This equation is split into  $N$  independent equations, one for each critical speed

$$\vec{\phi}_n^T \vec{U}_C = -\vec{\phi}_n^T \vec{U}_I, \quad n = 1 \dots N. \quad (8)$$

The initial unbalance  $\vec{U}_I$  is usually unknown. Practical modal balancing facilitates the fact that at a resonance point the according mode shape is dominant [13].

As long as the system is linear, the proposed method can calculate the amount of imbalance at a single point of the rotor, which leads to the same response as the distributed unbalance of the real system at one specific critical speed

$$U_{\text{gen}}^j = \frac{1}{M} \sum_{k=1}^M \frac{A_I^{jk}}{A_S^{jk}}, \quad (9)$$

where  $j$  is the index of the critical speed and  $M$  is the number of measurement positions [2]. The solution of equation (9) is used as the starting value for a solver that minimizes the error across all measured positions according to the least squares method. Usually this generalised unbalance  $\vec{U}_{\text{gen}}$  has a different amount and direction for every critical speed and quantifies how much a mode shape is excited by the initial unbalance. If the generalised unbalance for the first mode shape is mounted on the opposite side of the rotor, the vibration at the first critical speed is minimized, but the unbalance response at any other critical speed is also influenced.

To solve the problem that every set of balancing weights also influences all other modes, the generalised imbalances are computed with the modal matrix to generate orthogonal balancing weights

$$\vec{U}_C^j = -(\vec{\phi}_j^T)^{-1} (\vec{\phi}_j^T \vec{U}_{\text{gen}}). \quad (10)$$

Each of these sets of weights balances a single mode without influencing the others. Thus it is possible to balance the first  $N$

critical speeds of the rotor-bearing system so that the operating speed can be reached. If  $N \rightarrow \infty$ , the system is completely balanced. In this case the relation

$$\vec{U}_I = -\sum_{j=1}^N \vec{U}_C^j \quad (11)$$

is valid [13]. The correction weights are mounted on the rotor by adding weights at the balancing positions. It is also possible – although rarely done – to remove the same amount of mass from the opposite direction of the rotor. In the case of the following experiments, the initial rotor is simulated using ANSYS® 2019R2, therefore the balancing weights are mounted by adding centrifugal forces to the system parameters. The balancing success is evaluated by comparing the amplitude of the vibration of the original and the balanced system at every critical speed and every measurement position. The average of these values is called the balancing success rate.

## 3. EXPERIMENTS

To prove the viability of the balancing method, it is used on three numeric simulations of rotor-bearing systems. For every experiment the balancing success rate, the calculated balancing weights and the Frequency Response Functions (FRFs) – of the initial and the balanced state of the rotor – are shown. The displacements of the FRFs are the average values of the vibration amplitude of all measurement positions. All calculations are performed on an Intel® Core™ i7-8700 CPU with 3.2 GHz running on a Windows 10 operating system. Due to small differences between the NAT and the numerical ANSYS® 2019R2 calculation, the critical speeds calculated by the search algorithm may differ from the critical speeds visible in the FRFs.

### 3.1. Example 1: Three-disc rotor in rigid bearings

The first example consists of a thin rotor with three discs of different weight. The setup is shown in Fig. 4. The parameters to describe the stations of the NAT model are shown in Table 1. All segments have a density of 7800 kg/m<sup>3</sup>, a Young's modulus of 2.1 · 10<sup>11</sup> N/m<sup>2</sup> and a diameter of 30 mm.

As a first step, the critical speeds of the system are calculated using the recursive search algorithm. The eigenvalues are found

**Table 1**  
Stations of example 1

| $z$<br>(m) | $m_d$<br>(kg) | $\Theta$<br>(kg m <sup>2</sup> ) | $\Theta_{zz}$<br>(kg m <sup>2</sup> ) | $\varepsilon$<br>(μm) | $\beta$<br>(rad) | $c$<br>(N/m)    | $d$<br>(Ns/m) |
|------------|---------------|----------------------------------|---------------------------------------|-----------------------|------------------|-----------------|---------------|
| 0          | 0             | 0                                | 0                                     | 0                     | 0                | 0               | 0             |
| 0.13       | 0             | 0                                | 0                                     | 0                     | 0                | 10 <sup>7</sup> | 0             |
| 0.31       | 25            | 0.013                            | 0.026                                 | 20                    | 0                | 0               | 0             |
| 0.47       | 20            | 0.01                             | 0.02                                  | 25                    | 0.5 · π          | 0               | 0             |
| 0.71       | 15            | 0.008                            | 0.016                                 | 80                    | π                | 0               | 0             |
| 0.91       | 0             | 0                                | 0                                     | 0                     | 0                | 10 <sup>7</sup> | 0             |
| 1.04       | 0             | 0                                | 0                                     | 0                     | 0                | 0               | 0             |

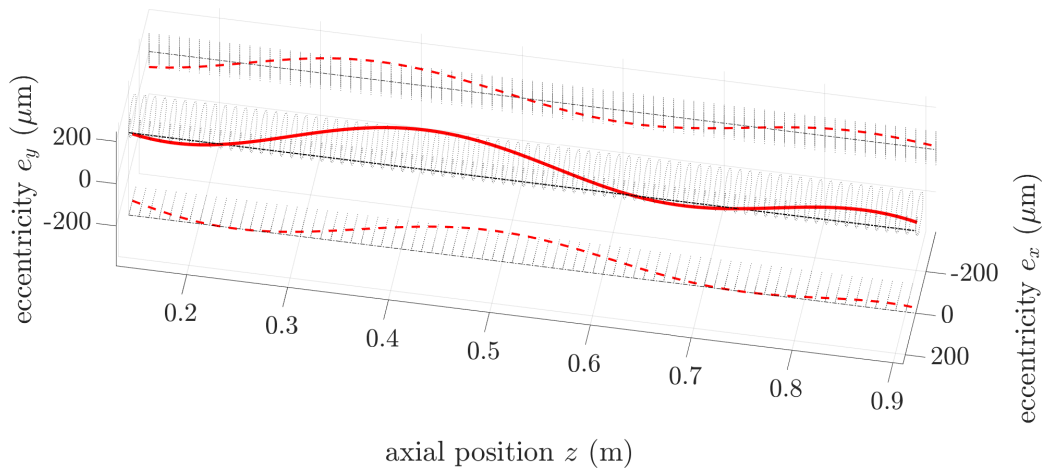


Fig. 3. Visualisation of distributed eccentricity

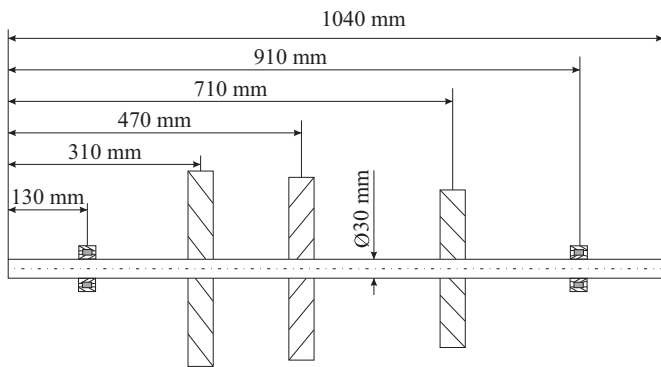


Fig. 4. Rotor-bearing system, example 1

in 0.56 seconds. Since the system is only balanced in the first three bending modes, only the first three critical speeds at 1347 rotations per minute (rpm), 5124 rpm and 11140 rpm are important. The measure and balancing positions are the planes of the three discs. The software computes the results in 0.189 seconds. It estimates the balancing weights as is shown in Table 2. This matches the initial unbalance rotated by 180°. In this simple example the vibrations are nearly completely eliminated. The balancing success rate is at 99.99%. In Fig. 5 the FRFs of the balanced and the unbalanced system are shown.

Since the unbalance is concentrated only in the three discs, it is sufficient to balance those three positions (at the first three critical speeds) to evaluate the initial unbalance and balance the system completely. Therefore, the vibrations of the fourth and the fifth mode are also reduced.

Table 2  
Balancing weights of example 1

| axial position (m) | amount (g mm) | angular position (°) |
|--------------------|---------------|----------------------|
| 0.31               | 500           | 180.00               |
| 0.47               | 500           | 269.95               |
| 0.71               | 1200          | 359.99               |

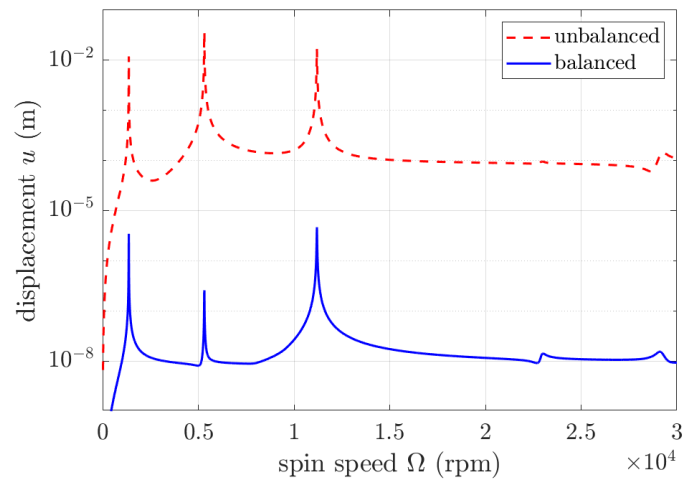


Fig. 5. FRFs of example 1

### 3.2. Example 2: Rotor with stepped shaft and elastic bearings

In example 2, the mass is not primarily concentrated at discs, but distributed along a stepped shaft. The diameter changes according to Fig. 6. The bearings are isotropic and flexible compared to the rotor with a spring constant of 600 kN/m and a damping constant of 80 Ns/m. The imbalance is distributed like a corkscrew along the area between the bearings as is seen

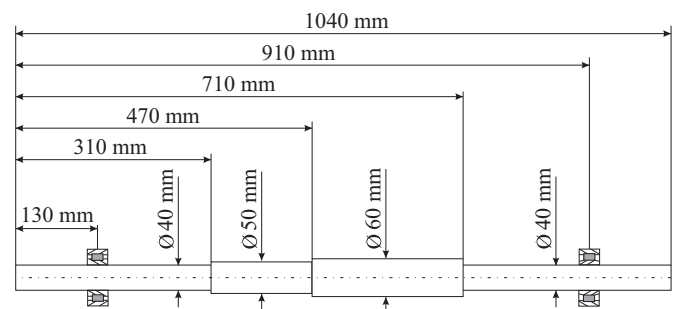


Fig. 6. Rotor-bearing system, example 2



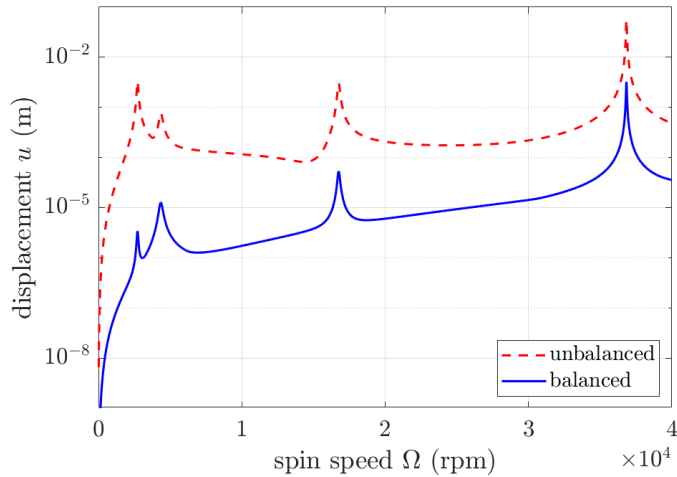


Fig. 7. FRFs of example 2

Table 3  
Balancing weights of example 2

| axial position (m) | amount (g mm) | angular position ( $^\circ$ ) |
|--------------------|---------------|-------------------------------|
| 0.31               | 157           | 29.10                         |
| 0.47               | 847           | 297.88                        |
| 0.59               | 976           | 90.64                         |
| 0.71               | 397           | 299.14                        |

in Fig. 3. This is assumed to be the most challenging case to balance [18]. For this example a magnitude of eccentricity of

$$\varepsilon = -0.007z^4 + 0.012z^3 + 0.005z^2 + 3 \cdot 10^{-4}z + 2 \cdot 10^{-4} \quad (12)$$

and a direction of imbalance of

$$\beta = 2\pi \cdot z \quad (13)$$

have been arbitrarily chosen. The first four eigenvalues are found by the recursive 2D search algorithm at 2723 rpm, 3987 rpm, 14 392 rpm and 30 317 rpm. The balancing positions are at 0.31 m, 0.47 m, 0.59 m and 0.71 m. The system is balanced in 0.187 seconds with a success rate of 95.13%. The calculated compensation unbalances are shown in Table 3. The first two mode shapes are the mode shapes of the elastic bearings, where little flexural displacement of the rotor occurs. The third and the fourth mode shape of the system are the first and second flexural mode shape of the rotor. In Fig. 7, the depicted FRFs show that all four modes are balanced.

### 3.3. Example 3: Three-disc rotor with stepped shaft in three bearings

The third example combines the three discs of the first example with the stepped shaft and distributed unbalance of the second example. The rotor is constrained by three rigid, damped and isotropic bearings as is shown in Fig. 8. The first five eigenvalues are 4516 rpm, 8964 rpm, 18910 rpm, 22164 rpm and 30220 rpm and the balancing positions are 0.31 m, 0.39 m, 0.47 m,

Table 4  
Balancing weights of example 3

| axial position (m) | amount (g mm) | angular position ( $^\circ$ ) |
|--------------------|---------------|-------------------------------|
| 0.31               | 357           | 95.49                         |
| 0.39               | 1365          | 224.42                        |
| 0.47               | 1294          | 356.88                        |
| 0.65               | 735           | 135.14                        |
| 0.71               | 1698          | 346.82                        |

0.65 m and 0.71 m. The example is balanced in 0.202 seconds with a success rate of 97.58%. The compensation unbalance is approximated according to Table 4. The FRFs in Fig. 9 show that the system is balanced throughout all speeds.

To show the effect of measurement uncertainties, example 3 is balanced again, but this time each amplitude of the unbalance response in  $x$ - and  $y$ -direction is multiplied with a uniformly distributed random number between 0.95 and 1.05. Despite the added noise, these tests result in a balancing success rate of 96.26% (average of ten tests). The specifics and the balancing success of every example are shown in Table 5.

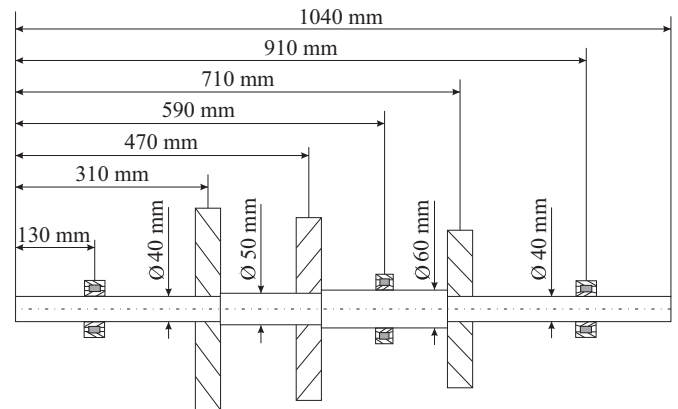


Fig. 8. Rotor-bearing system, example 3

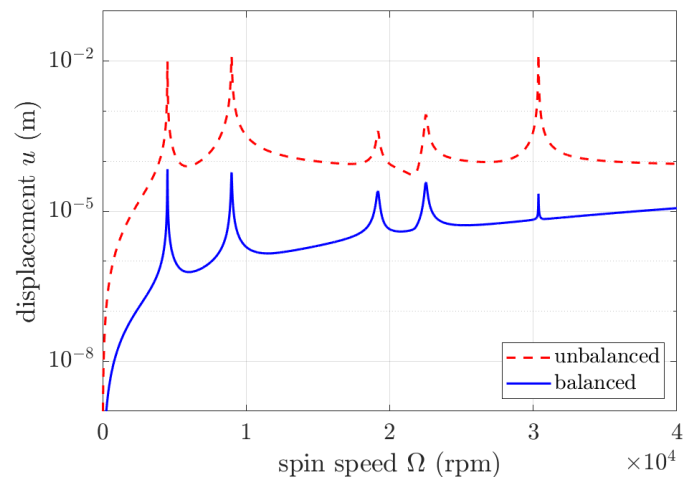


Fig. 9. FRFs of example 3

**Table 5**  
Summary of results

| example | imbalance    | bearings  | damping  | balancing success |
|---------|--------------|-----------|----------|-------------------|
| 1       | concentrated | 2 rigid   | undamped | 99.99%            |
| 2       | distributed  | 2 elastic | damped   | 95.13%            |
| 3       | distributed  | 3 rigid   | damped   | 97.58%/96.26%     |

#### 4. CONCLUSION

The proposed balancing method is successfully applied in three different test cases. The influence of multiple discs, multiple bearings, stepped shafts, arbitrarily distributed unbalance and external damping are taken into account. The method can only be properly applied on isotropic rotor-bearing systems, the extension to anisotropic systems is the focus of further research. The simulation via NAT is computationally efficient, with computation times below one second for all three tests. Systems with concentrated unbalance are ideally balanced as is shown in example 1. For complex systems with distributed unbalance and noise, success rates of more than 95% are achieved in examples 2 and 3. Recursive search algorithms are well suited to find eigenvalues of the system matrix of NAT. The results indicate that the proposed balancing method can be applied effectively.

#### ACKNOWLEDGEMENTS

The authors acknowledge the financial support by the Graz University of Technology Open Access Publishing Fund.

#### REFERENCES

- [1] J. Tessarzik, *Flexible rotor balancing by the exact point speed influence coefficient method*. Latham: Mechanical Technology Incorporated, 1972.
- [2] P. Gnielka, "Modal balancing of flexible rotors without test runs: An experimental investigation," *Journal of Vibrations*, vol. 90, no. 2, pp. 152–170, 1982.
- [3] K. Federn, "Grundlagen einer systematischen Schwingungsstörung wellenelastischer Rotoren," *VDI Bericht*, vol. 24, pp. 9–25, 1957.
- [4] A. G. Parkinson and R. E. D. Bishop, "Residual vibration in modal balancing," *Journal of Mechanical Engineering Science*, vol. 7, pp. 33–39, 1965.
- [5] W. Kellenberger, "Das Wuchten elastischer Rotoren auf zwei allgemein-elastischen Lagern," *Brown Boveri Mitteilungen*, vol. 54, pp. 603–617, 1967.
- [6] A.-C. Lee, Y.-P. Shih, and Y. Kang, "The analysis of linear rotor bearing systems: A general Transfer Matrix Method," *Journal of Vibration and Acoustics*, vol. 115, no. 4, pp. 490–497, 1993.
- [7] J.-S. Wu and H. M. Chou, "A new approach for determining the natural frequency of mode shapes of a uniform beam carrying any number of sprung masses," *Journal of Sound and Vibration*, vol. 220, no. 3, pp. 451–468, 1999.
- [8] J.-S. Wu, F.-T. Lin, and H.-J. Shaw, "Analytical solution for whirling speeds and mode shapes of a distributed-mass shaft with arbitrary rigid disks," *Journal of Applied Mechanics*, vol. 81, no. 3, pp. 034 503–1–034 503–10, 2014.
- [9] M. Klanner, M.S. Prem, and K. Ellermann, "Steady-state harmonic vibrations of a linear rotor-bearing system with a discontinuous shaft and arbitrarily distributed mass unbalance," in *Proceedings of ISMA2020 International Conference on Noise and Vibration Engineering and USD2020 International Conference on Uncertainty in Structural Dynamics*, 2020, pp. 1257–1272.
- [10] M. Klanner and K. Ellermann, "Steady-state linear harmonic vibrations of multiple-stepped Euler-Bernoulli beams under arbitrarily distributed loads carrying any number of concentrated elements," *Applied and Computational Mechanics*, vol. 14, no. 1, pp. 31–50, 2019.
- [11] M.B. Deepthikumar, A.S. Sekhar, and M.R. Srikanthan, "Modal balancing of flexible rotors with bow and distributed unbalance," *Journal of Sound and Vibration*, vol. 332, pp. 6216–6233, 2013.
- [12] O.A. Bauchau and J.I. Craig, *Structural Analysis – With Applications to Aerospace Structures*. Heidelberg: Springer Verlag, 2009.
- [13] R.E.D. Bishop and A.G. Parkinson, "On the isolation of modes in balancing of flexible shafts," *Proc. Inst. Mech. Eng.*, vol. 117, pp. 407–426, 1963.
- [14] X. Rui, G. Wang, Y. Lu, and L. Yunm, "Transfer Matrix Method for linear multibody systems," *Multibody Syst. Dyn.*, vol. 19, pp. 179–207, 2008.
- [15] I.N. Bronstein, K.A. Semendjajew, and E. Zeidler, *Taschenbuch der Mathematik*. Stuttgart: Teubner, 1996.
- [16] D. Bestle, L. Abbas, and X. Rui, "Recursive eigenvalue search algorithm for transfer matrix method of linear flexible multibody systems," *Multibody Syst. Dyn.*, vol. 32, pp. 429–444, 2013.
- [17] B. Xu and L. Qu, "A new practical modal method for rotor balancing," *Proc. Inst. Mech. Eng. Part C J. Mech. Eng. Sci.*, vol. 215, pp. 179–190, 2001.
- [18] J. Tessarzik, *Flexible rotor balancing by the influence coefficient method. Part 1: Evaluation of the exact point speed and least squares procedure*. Latham: Mechanical Technology Incorporated, 1972.